Supporting Information

Selective CO_2 reduction to HCOOH on a $Pt/In_2O_3/g\text{-}C_3N_4$ multifunctional visible-photocatalyst

Jiehong He, Pin Lv, Jian Zhu*, Hexing Li*

Education Ministry Key and International Joint Lab of Resource Chemistry and Shanghai Key Laboratory of Rare Earth Functional Materials, Department of Chemistry, Shanghai Normal University, Shanghai 200234, China.

*Corresponding authors. Tel: +86 21 64322272; Fax: +86 21 64322272.

E-mail address: hexing-li@shnu.edu.cn (Hexing Li)

jianzhu@shnu.edu.cn (Jian Zhu)

Table S1 Theoretical and real In_2O_3-content and Pt-loading in mass percentage.

Sample	In_2O_3-content (%)		Pt-loading (%)	
	Theoretical	Real	Theoretical	Real
2Pt-In_2O_3	98.04	/	1.96	1.92
2Pt-g-C_3N_4	0	0	1.96	1.98
1Pt-10INCN	9.09	8.88	0.99	0.87
1.5Pt-10INCN	9.09	9.13	1.48	1.45
2Pt-10INCN	9.09	9.03	1.96	1.95
2.5Pt-10INCN	9.09	8.95	2.44	2.46
2Pt-5INCN	4.76	4.51	1.48	1.44
2Pt-15INCN	13.04	13.12	1.48	1.51
2Pt-20INCN	16.67	16.51	1.48	1.32
2Pt-10INCN-mix	9.09	9.12	1.48	1.44

Table S2 Structural parameters determined from N_2 adsorption-desorption isotherms.

Catalyst	Surface area (m^2/g)	Pore Size (nm)	Pore volume (cm^3/g)
In_2O_3	31.18	21.18	0.039
g-C_3N_4	14.02	19.31	0.043
5INCN	32.51	11.97	0.169
10INCN	25.32	13.29	0.104
15INCN	23.84	15.82	0.170
20INCN	28.36	12.67	0.109
1Pt-10INCN	15.66	21.70	0.066
1.5Pt-10INCN	13.27	22.20	0.074
2Pt-10INCN	13.10	22.86	0.075
2.5Pt-10INCN	7.642	27.28	0.052
2Pt- In_2O_3	10.33	24.06	0.061
2Pt- g-C_3N_4	6.980	27.58	0.048
2Pt-5INCN	18.64	23.95	0.112
2Pt-15INCN	11.20	22.60	0.065
2Pt-20INCN	11.03	22.01	0.073
2Pt-10INCN-mix	5.365	29.25	0.039

Table S3 Energy bandgap (Eg) and calculated light absorbance edge wavelength (λ).

Catalyst	Eg/eV	λ/nm
g-C_3N_4	2.83	438
In_2O_3	2.91	426
5INCN	2.74	453
10INCN	2.75	451
15INCN	2.76	449
20INCN	2.77	448
2Pt-g-C_3N_4	2.73	454
2Pt-In_2O_3	2.78	446
2Pt-5INCN	2.68	463
2Pt-10INCN	2.65	468
2Pt-15INCN	2.62	473
2Pt-20INCN	2.62	473

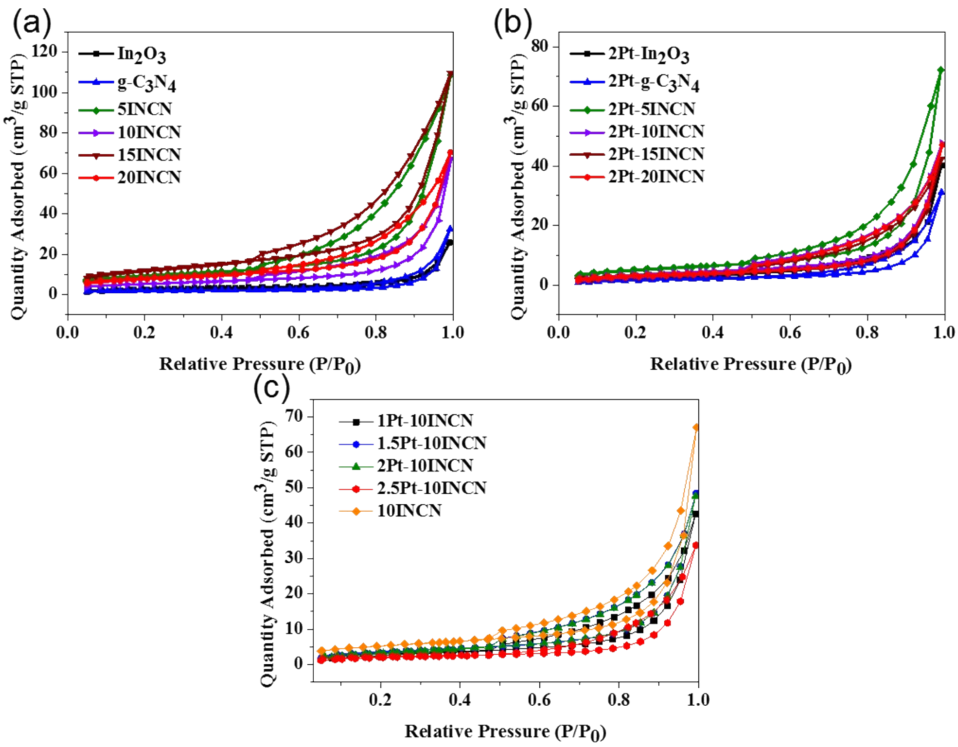

Fig. S1 N_2 adsorption-desorption isotherms of pure In_2O_3, pure g-C_3N_4 and their corresponding composites with or without Pt-loading.

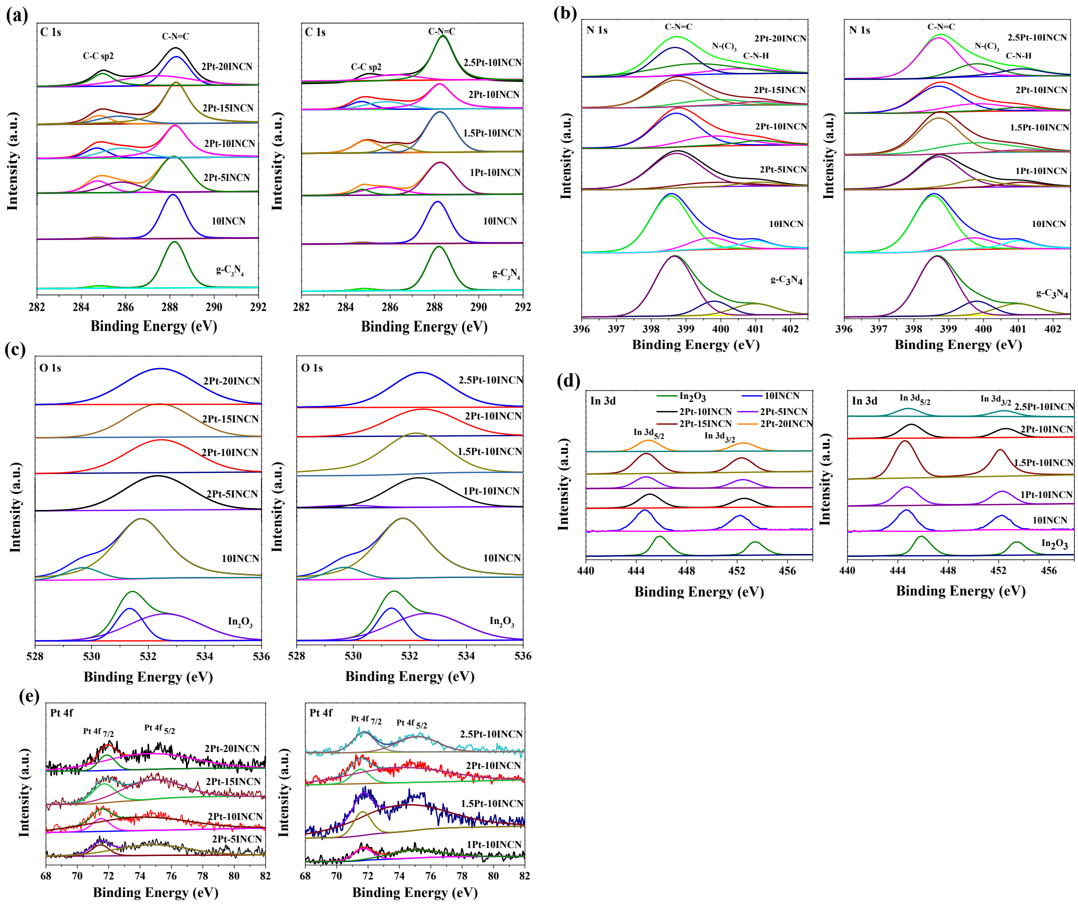

Fig. S2 XPS spectra in (a) C 1s, (b) N 1s, (c) O 1s, (d) In 3d, and (e) Pt 4f levels.

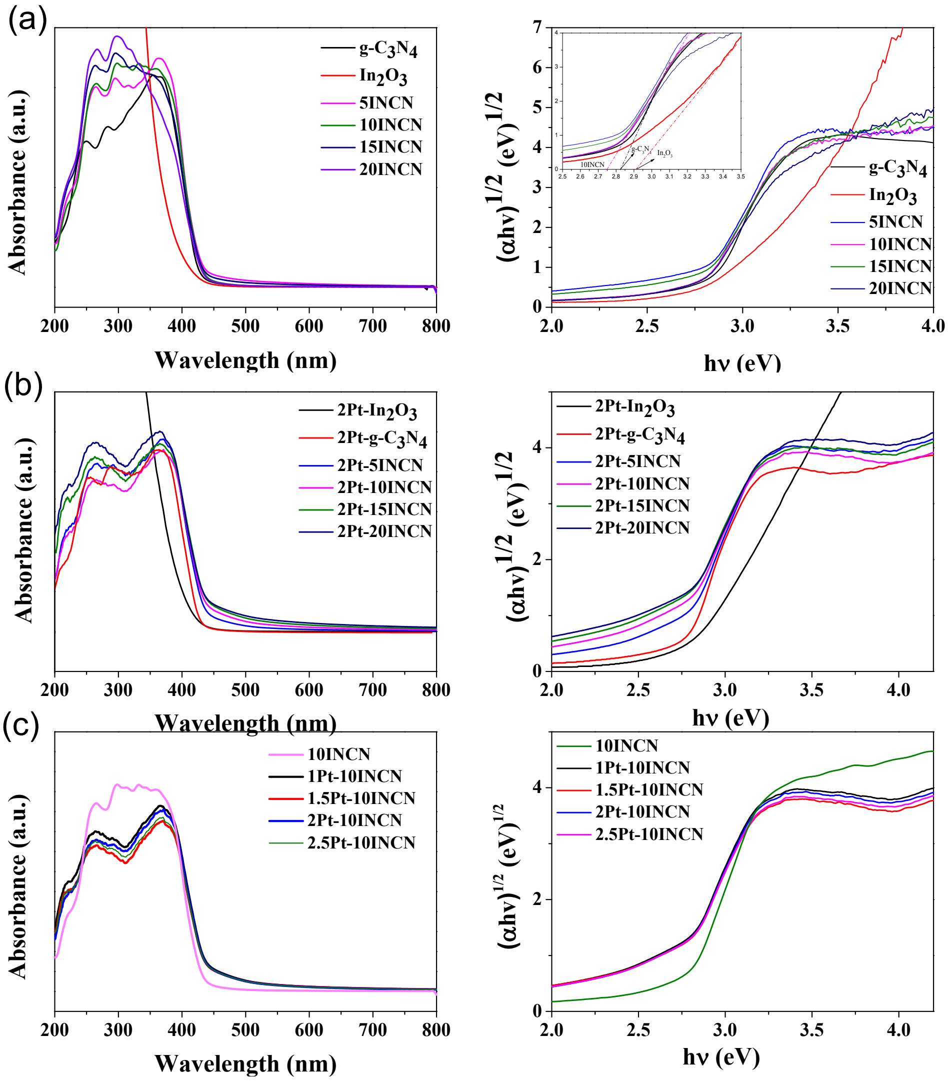

Fig. S3 UV-Vis DRS spectra and plots of $(\alpha h\nu)^{1/2}$ *vs.* photon energy (hν).

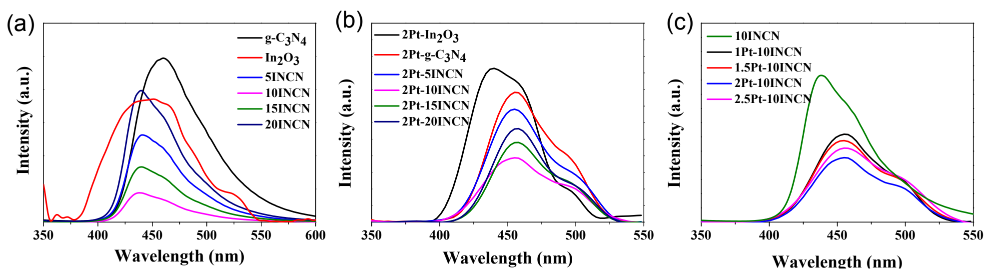

Fig. S4 PL spectra obtained at λ_{ex} of 350 nm.

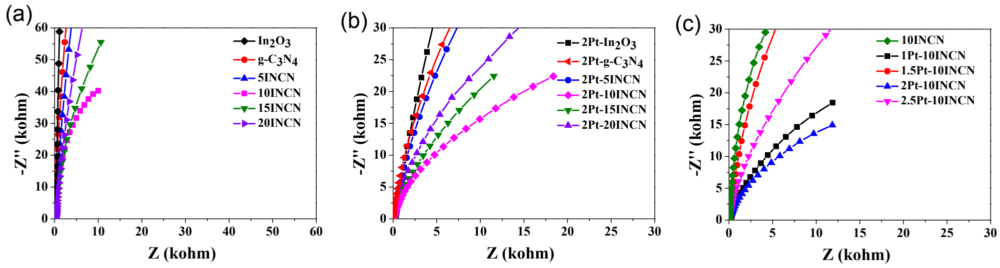

Fig. S5 Electrochemical impedance spectra.

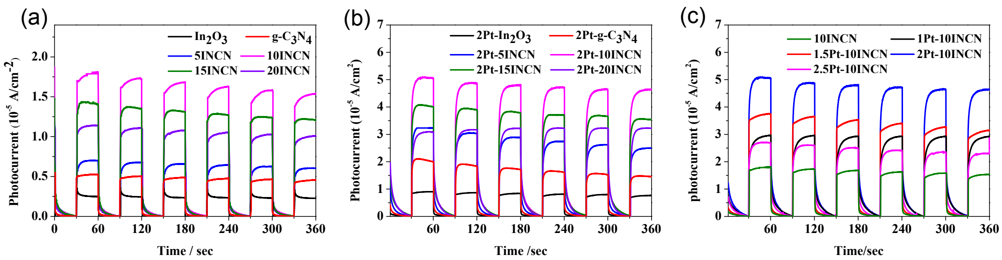

Fig. S6 Photocurrent response spectra obtained under irradiation of a 300 W Xe lamp.

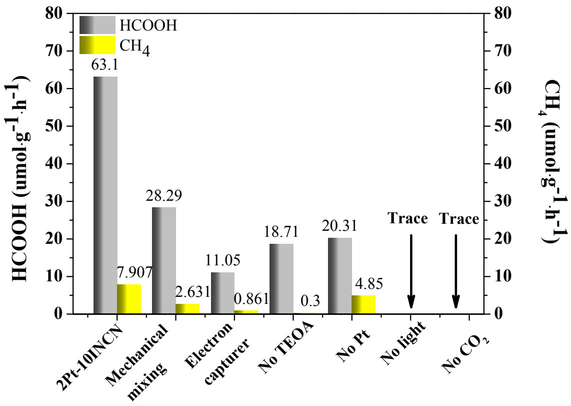

Fig. S7 Controlled experiments for the photocatalytic CO_2 reduction on 2Pt-10INCN. Reaction conditions: Four 3 W LED (420 nm), 35°C, 1 atm CO_2, 20 mg catalyst, 10 mL H_2O, 1 mL TEOA, 4 h.

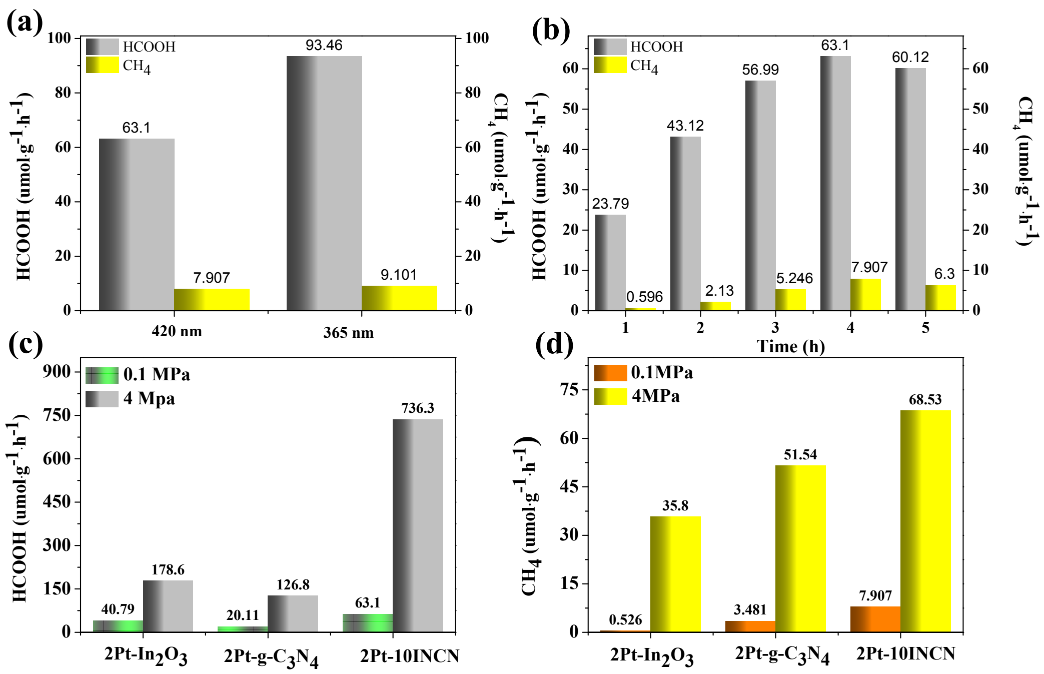

Fig. S8 Effects of light source (a), reaction time (b) and CO_2 pressure (c, d) on the HCOOH and CH_4 yield during CO_2 photocatalytic reduction with different catalysts. Other reaction conditions are given in Fig. S7.

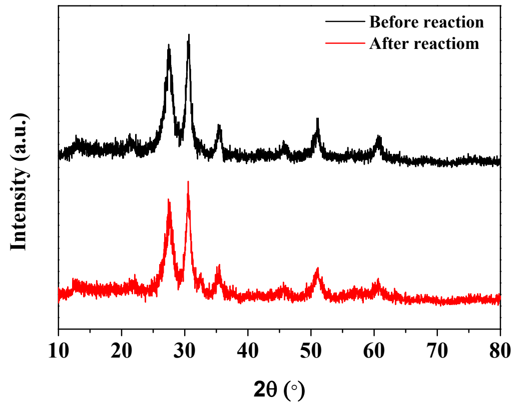

Fig. S9 XRD patterns of 2Pt-10INCN before and after recycling reactions

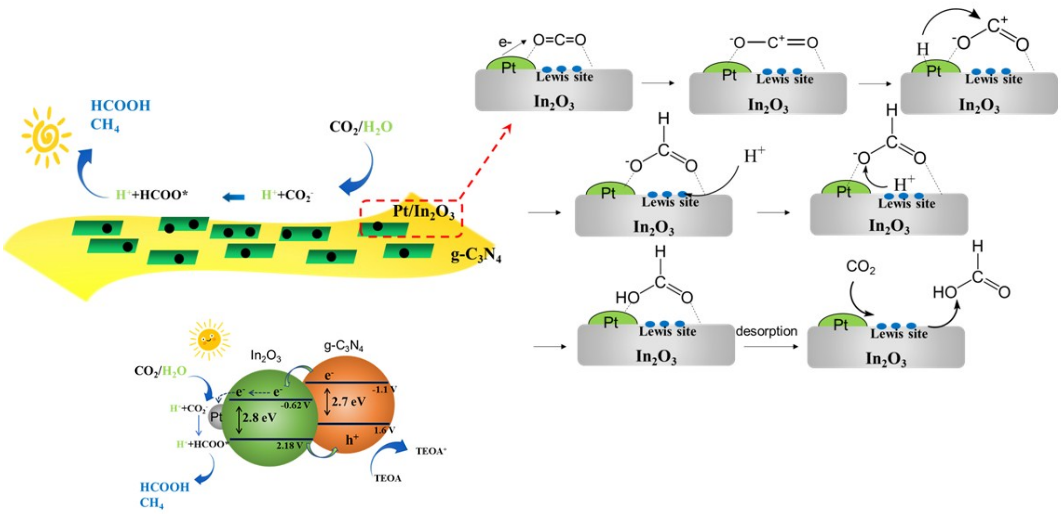

Scheme S1 A plausible reaction pathway for photocatalytic CO_2 reduction to HCOOH on Pt-INCN.